

hsa_circ_0038382 upregulates T-box transcription factor 5 to inhibit keloid formation by interacting with miR-940

*Meihong Cai^{1,A,C,D}, *Zhen Hu^{2,C-E}, Lin Liu^{3,B,D,E}, Jiangwei Su^{3,E,F}

¹ Department of Dermatology, Wuhan Wuchang Hospital, Wuchang Hospital Affiliated to Wuhan University of Science and Technology, China

² Department of Dermatology, Wuhan Third Hospital, China

³ Department of Dermatology, Ezhou Central Hospital, China

A – research concept and design; B – collection and/or assembly of data; C – data analysis and interpretation;

D – writing the article; E – critical revision of the article; F – final approval of the article

Advances in Clinical and Experimental Medicine, ISSN 1899–5276 (print), ISSN 2451–2680 (online)

Adv Clin Exp Med. 2023;32(5):593–601

Address for correspondence

Jiangwei Su

E-mail: SuJiangwei3@163.com

Funding sources

None declared

Conflict of interest

None declared

* Meihong Cai and Zhen Hu contributed equally to this work.

Received on April 15, 2022

Reviewed on September 30, 2022

Accepted on October 21, 2022

Published online on November 22, 2022

Abstract

Background. A keloid is a benign fibroproliferative skin tumor whose formation is regulated by circular RNAs (circRNAs). However, the effect and regulatory mechanism of hsa_circ_0038382 on keloid formation have not been investigated.

Objectives. This study aimed to identify the function and mechanism of hsa_circ_0038382 in keloid formation.

Materials and methods. The expression levels of hsa_circ_0038382, microRNA-940 (miR-940) and T-box transcription factor 5 (*TBX5*) were measured using real-time quantitative reverse transcription polymerase chain reaction (qRT-PCR). After cell transfection of keloid fibroblasts, the effect of the hsa_circ_0038382/miR-940/*TBX5* axis on keloid formation was assessed using cell function tools such as the cell counting kit-8 (CCK-8) assay, transwell migration assay and transwell invasion assay. The binding sites among hsa_circ_0038382, miR-940 and *TBX5* were predicted with CircInteractome and TargetScan, and further identified using luciferase assays.

Results. The levels of hsa_circ_0038382 and *TBX5* were reduced, whereas the level of miR-940 was elevated in keloid samples. Cell function experiments confirmed that hsa_circ_0038382 can inhibit keloid formation by suppressing proliferation, migration and invasion of keloid fibroblasts. Luciferase assays proved that hsa_circ_0038382 can absorb miR-940 to regulate *TBX5* expression in keloids. Additionally, the overexpression of *TBX5* restored the effect of hsa_circ_0038382 knockdown on keloid fibroblasts.

Conclusions. This study suggests that hsa_circ_0038382 attenuates keloid formation by regulating the miR-940/*TBX5* axis, which might provide a potential therapeutic target in the treatment of keloid formation.

Key words: keloid, hsa_circ_0038382, miR-940, *TBX5*

Cite as

Cai M, Hu Z, Liu L, Su J. hsa_circ_0038382 upregulates T-box transcription factor 5 to inhibit keloid formation by interacting with miR-940. *Adv Clin Exp Med*. 2023;32(5):593–601. doi:10.17219/acem/155949

DOI

10.17219/acem/155949

Copyright

Copyright by Author(s)

This is an article distributed under the terms of the Creative Commons Attribution 3.0 Unported (CC BY 3.0) (<https://creativecommons.org/licenses/by/3.0/>)

Background

A keloid, characterized by the hyperproliferation of fibroblasts and abnormal deposition of collagen fibers, is a benign fibroproliferative skin tumor.^{1,2} Keloid formation is caused by cutaneous injuries, including trauma, burns and surgery,³ and involves multiple regulators, including cytokines, gene regulators and inflammatory factors.⁴ The overproliferation of fibroblast, overproduction of collagen and abnormal extracellular matrix remodeling are key factors in keloid formation.⁵ For keloid therapy, the mainstay of treatment is conservative therapy, such as surgery alone or in combination with depot steroids. However, a high recurrence rate often leads to unsatisfactory outcomes.^{6,7} Hence, an in-depth investigation of the mechanisms behind keloid formation is urgently required for keloid treatment.

Circular RNAs (circRNAs), which are non-coding RNAs, are more stable than linear RNAs because they form a continuous circle.⁸ Accumulating evidence reveals that aberrantly expressed circRNAs in keloids play key roles in regulating keloid formation.^{9–11} For example, circRNA nuclear receptor-interacting protein 1 (circNRIP1) is overexpressed in keloid tissues, and the downregulation of circNRIP1 expression inhibited the proliferation of keloid-derived fibroblasts.¹⁰ The overexpression of another circRNA, circ_101238, has been shown to promote the proliferation and inhibit the apoptosis of keloid fibroblasts.⁹ We identified a novel circRNA, hsa_circ_0038382, by analyzing a keloid circRNA microarray from the Gene Expression Omnibus (GEO) database. Because of the lack of knowledge regarding the effects of hsa_circ_0038382 on keloids, this study is the first to investigate the function of hsa_circ_0038382 in keloids.

The circRNAs that interact with microRNAs (miRNAs) to regulate downstream target genes have been confirmed in multiple human diseases, such as cancer, osteoporosis and cardiac hypertrophy.^{12–14} In keloids, circRNA protein tyrosine phosphatase non-receptor type 12 (PTPN12) has been reported to target the miR-21-5p/*SMAD7* axis, thereby inhibiting keloid fibroblast growth.¹⁵ Our study predicted that miR-940 might be the downstream miRNA of hsa_circ_0038382 using CircInteractome (<https://circinteractome.nia.nih.gov/>) analysis. The miR-940 has been reported as a tumor promoter in breast cancer¹⁶ and endometrial carcinoma,¹⁷ and as an antitumor factor in non-small cell lung carcinoma¹⁸ and esophageal squamous cell carcinoma.¹⁹ However, the effects of miR-940 on keloids remain unknown. Here, we explored the influence of miR-940 and the interaction between hsa_circ_0038382 and miR-940 on keloids.

T-box transcription factor 5 (*TBX5*), containing a DNA-binding domain T-box sequence, can induce cell apoptosis.²⁰ Previous studies have confirmed the antitumor function of *TBX5* in colon cancer,²¹ non-small cell lung carcinoma²² and cutaneous melanoma.²³ Nevertheless, the mechanism of action of *TBX5* in keloids remains unclear. Using TargetScan (<https://www.targetscan.org>), *TBX5* was predicted

to be the target gene of miR-940; however, the relationship between *TBX5* and miR-940 has not been reported. Therefore, we explored the function and mechanism of action of *TBX5* in keloids.

Objectives

Based on a bioinformatic analysis and a literature review, we speculated that hsa_circ_0038382 might affect keloid formation through the miR-940/*TBX5* axis. Therefore, the present study aimed to identify the function of the hsa_circ_0038382/miR-940/*TBX5* axis on keloids, and assess whether it could be a novel therapeutic target for keloid treatment.

Materials and methods

Microarray analysis

The GSE184097 from the GEO database is a circRNA expression microarray containing keloid and normal skin samples. The ASCRP3013082 is the ID of hsa_circ_0038382 in GSE184097. The GEO2R was used to identify hsa_circ_0038382 expression in keloids and normal skin samples. The binding sites of hsa_circ_0038382, miR-940 and *TBX5* were predicted using CircInteractome and TargetScan.

Clinical sample collection

Keloids and paired normal skin tissues (>5 cm from the keloid) were collected from 28 patients in our hospital. None of the patients had received radiotherapy, chemotherapy or laser treatment before surgery. Our study was approved by the Ethics Committee of Wuhan Wuchang Hospital, China (approval No. 2022006). All patients signed an informed consent form. The clinical characteristics of the patients are presented in Table 1.

Real-time quantitative reverse transcription polymerase chain reaction (qRT-PCR)

Total RNA was isolated using RNAiso Plus (TaKaRa, Tokyo, Japan), and miRNA was isolated using the miRNeasy FFPE Kit (BioTeke, Wuxi, China). Reverse transcription was performed using a PrimeScript RT kit (TaKaRa). Real-time quantitative reverse transcription polymerase chain reaction was performed using SYBRTM Green PCR Master Mix (TaKaRa) with the following primer sequences: hsa_circ_0038382: forward, 5'-CGGGCCTATATGGAGAA-CAA-3' and reverse, 5'-TCTCTCCTCACTGCCCAACT-3'; miR-940: forward, 5'-GTATAAAGGGCCCCCGCT-3' and reverse, 5'-AGGGTCCGAGGTATTCGCACT-3'; and *TBX5*: forward, 5'-CTCAAGCTCACCAACAACCA-3' and

Table 1. Clinical characteristics of 28 patients with keloid

Variable	Number (total = 28)
Age, median (range) [years]	36 (26–48)
Sex	
Male, n	13
Female, n	15
Number of keloid nodules	
1	11
2–4	9
≥5	8
Location	
Face, neck	5
Trunk, shoulder	17
Extremities	6
Symptom	
Itching	10
Pain	1
Itching & pain	17

reverse, 5'-CAGGAAAGACGTGAGTGCAG-3'. The relative expression was calculated using the $2^{-\Delta\Delta CT}$ method²⁴ with glyceraldehyde 3-phosphate dehydrogenase (*GAPDH*) and U6 as internal references.

Cell culture and transfection

Human keloid fibroblasts (HKFs; CP-H235) were purchased from Procell Life Science and Technology Co., Ltd. (Wuhan, China), whereas normal human dermal fibroblasts (HDFs; BNCC358600) were purchased from the BeNa Culture Collection (Beijing, China). All cells were cultured in Dulbecco's modified Eagle's medium (DMEM) containing 10% fetal bovine serum (FBS), 1% penicillin and 1% streptomycin under 5% CO₂ and at 37°C.

Silencing RNAs (siRNAs) targeting hsa_circ_0038382 (si-hsa_circ_0038382), negative control (NC) of siRNAs, miR-940 mimic, and mimic-NC were constructed by RiboBio (Guangzhou, China). The hsa_circ_0038382 and *TBX5* overexpression vectors were also constructed by RiboBio using pcDNA3.1-circRNA or pcDNA3.1 vectors. The corresponding empty vector (pcDNA3.1-circRNA or pcDNA3.1) was used as the NC of the overexpression vector. For cell transfection, the 50 nM vectors mentioned above were transfected into HKFs at 50% confluence. After transfection for 48 h, qRT-PCR was performed to assess the transfection efficiency.

CCK-8 assay

Human dermal fibroblasts were seeded in a 96-well cell culture plate (3000/well). After transfection for 0, 24, 48, and 72 h, 10 µL of cell counting kit-8 (CCK-8) solution (Dojindo, Kumamoto, Japan) was pipetted into each well

and incubated for another 2 h at 37°C. Finally, the optical density (OD) value was recorded at 450 nm using a microplate reader (YK-SY96A; Yunke, Beijing, China).

EdU assay

The 5-ethynyl-2'-deoxyuridine (EdU) assays were performed to assess cell proliferation using an EdU cell proliferation kit (Solarbio Science & Technology Co., Ltd., Beijing, China). Transfected HKFs (1×10^4 cells/well) were seeded in 96-well plates and incubated overnight. The next day, 100 µL of 50 µM EdU solution was added to the HKFs and incubated for 2 h. After washing the HKFs with phosphate-buffered saline (PBS), the cells were fixed with fixative, treated with 0.1% Triton X-100, washed with PBS, and incubated with 100 µL of Apollo staining reaction solution. Then, the cells were incubated with 100 µL of $1 \times$ Hoechst 33342. Finally, they were observed and photographed using a fluorescence microscope (Olympus BX51; Olympus Corp., Tokyo, Japan).

Transwell migration and invasion assays

Matrigel diluted with a serum-free medium at a ratio of 1:8 was added to the polycarbonate film and incubated overnight for the invasion assay, but not for the migration assay. After transfection, 1×10^5 HKFs were added to the upper chamber with 200 µL of serum-free medium. Simultaneously, 600 µL of medium containing 10% FBS was added to the lower chamber. After incubation for 24 h, migratory and invasive HKFs were fixed using 4% paraformaldehyde and stained with 0.05% crystal violet. The cells were observed under an optical microscope (Olympus CX21; Olympus Corp., Tokyo, Japan). The number of cells was calculated in 5 random fields in each transwell chamber using ImageJ software (National Institutes of Health, Bethesda, USA).

Luciferase assay

Wild-type vectors of hsa_circ_0038382/*TBX5* (hsa_circ_0038382-WT/*TBX5*-WT) and mutant vectors of hsa_circ_0038382/*TBX5* (hsa_circ_0038382-MUT/*TBX5*-MUT) were constructed by RiboBio using pMIR-REPORT™ (Ambion, Austin, USA) vectors. Subsequently, each of the constructed luciferase reporter vectors was transfected into HKFs at 70% confluence along with miR-940 mimic or mimic-NC. After transfection for 48 h, luciferase activity was evaluated using a dual-luciferase reporter assay kit (Promega, Madison, USA).

Western blotting

Total protein was obtained from HKFs using a Total Protein Extraction Kit (PI250; Applygen Technologies Inc., Beijing, China). After determining the protein concentration with the aid of a BCA kit (Pierce, Rockford, USA), sodium

dodecyl-sulfate polyacrylamide gel electrophoresis (SDS-PAGE) gels (10%) were used to separate 20 µg of protein. The separated proteins were transferred onto polyvinylidene fluoride (PVDF) membranes. The membranes were blocked with 5% skim milk and incubated with TBX4 antibody (ab137833; Abcam, Cambridge, USA) or GAPDH antibody (ab9485; Abcam) at 4°C overnight, followed by the incubation with a fluorescent rabbit antibody (LI-COR Biosciences, Bad Homburg vor der Höhe, Germany) for 3 h at 37°C. The protein blots were acquired using Odyssey 3.2 (LI-COR Biosciences).

Statistical analyses

All experiments were performed in triplicate, and the data were analyzed using GraphPad Prism v. 8 (GraphPad Software, San Diego, USA) with a paired or unpaired Student’s t-test (between the 2 groups) or analysis of variance (ANOVA) test (>2 groups), followed by the Tukey’s multiple comparisons test. All data were identified as normally distributed using the Shapiro–Wilk test. Data are presented as a mean ± standard deviation (M ±SD). The value of p < 0.05 was considered statistically significant.

Results

hsa_circ_0038382 was downregulated in keloid

The GSE184097, a circRNA microarray, was downloaded from GEO DataSets, and differentially expressed

circRNAs were compared in keloid samples (n = 4) to normal skin samples (n = 4) with an adjusted p-value < 0.05 (Fig. 1A). In the GSE184097 microarray, GSM5577905, GSM5577906, GSM5577907, and GSM5577908 were the keloid samples, whereas GSM5577909, GSM5577910, GSM5577911, and GSM5577912 were the adjacent normal skin samples. The hsa_circ_0038382 expression was reduced in the 4 keloid samples compared to the 4 adjacent normal skin samples (Fig. 1B and Table 2). We collected keloid and adjacent normal tissues from 28 patients to identify the expression of hsa_circ_0038382 in our clinical samples. Our qRT-PCR data further showed that hsa_circ_0038382 levels were reduced by 50% in keloid tissues compared with paired normal skin tissues (Fig. 1C). Similarly, the expression of hsa_circ_0038382 in HKFs was downregulated by more than 50% compared to that in normal HDFs (Fig. 1D). The bioinformatics analysis and qRT-PCR experiments confirmed the downregulation of hsa_circ_0038382 in keloids.

Table 2. Sample values for hsa_circ_0038382 in GSE184097

Source	Sample	Value
Keloid dermal fibroblasts	GSM5577905	5.18
	GSM5577906	5.42
	GSM5577907	5.46
	GSM5577908	5.40
Normal dermal fibroblasts	GSM5577909	6.81
	GSM5577910	6.82
	GSM5577911	5.94
	GSM5577912	6.03

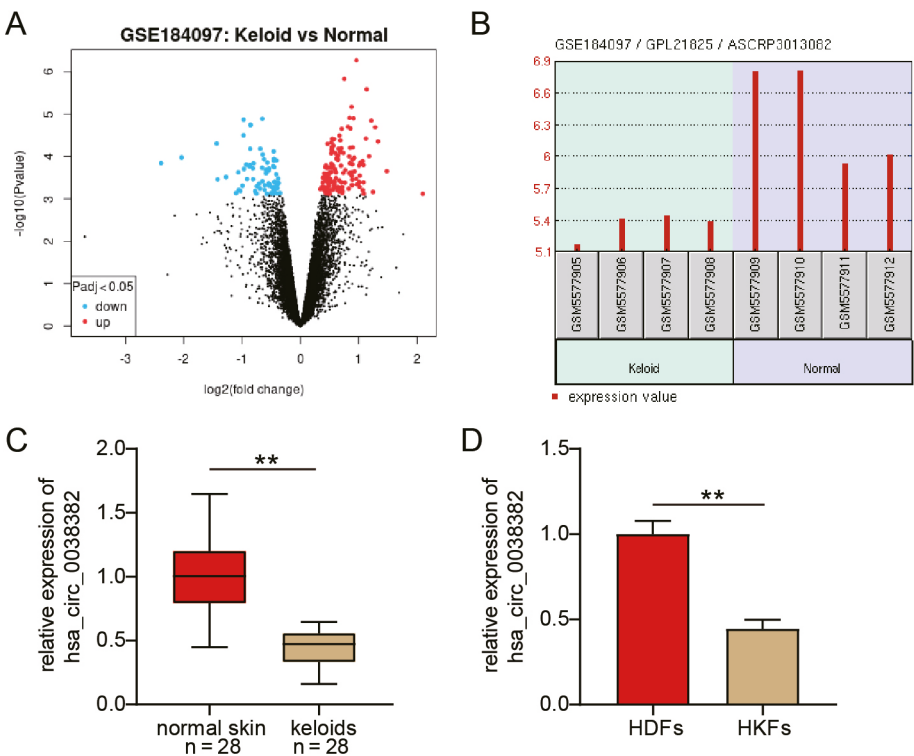


Fig. 1. The hsa_circ_0038382 was downregulated in keloid. A. Differentially expressed circular RNAs (circRNAs) in GSE184097; B. Downregulation of hsa_circ_0038382 in keloid samples; C. hsa_circ_0038382 expression was reduced in keloid tissues as identified using real-time quantitative reverse transcription polymerase chain reaction (qRT-PCR), n = 28; D. hsa_circ_0038382 expression was reduced in HKFs as identified using qRT-PCR

GSE184097 – circRNA microarray for keloid samples and normal skin samples; HDFs – normal human dermal fibroblasts; HKFs – human keloid fibroblasts; **p < 0.01.

hsa_circ_0038382 attenuates keloid formation in vitro

To verify the function of hsa_circ_0038382 in keloids, we transfected HKFs with hsa_circ_0038382 overexpression or knockdown vectors. The qRT-PCR was used to determine the transfection efficiency, which showed that the hsa_circ_0038382 overexpression vector induced > 6-fold increase in hsa_circ_0038382 expression in HKFs, and si-hsa_circ_0038382 caused a 70% decrease in its expression in HKFs (Fig. 2A). The CCK-8 assay demonstrated that the proliferation of HKFs was impaired in the hsa_circ_0038382 overexpression group, whereas it was enhanced in the si-hsa_circ_0038382 group (Fig. 2B). The EdU assay was used to confirm the change in the proliferation of transfected HKFs. The results revealed that the hsa_circ_0038382 overexpression vector led to >60% decrease in the EdU-positive rate, whereas hsa_circ_0038382 knockdown resulted in a 1.8-fold increase in the EdU-positive rate (Fig. 2C). Transwell migration and invasion assays revealed that the overexpression of hsa_circ_0038382 promoted migration and invasion of HKFs, whereas hsa_circ_0038382 knockdown inhibited the migration and invasion of HKFs (Fig. 2D). These data indicate that hsa_circ_0038382 attenuates keloid formation in vitro.

miR-940 targeted by hsa_circ_0038382 promotes HKF proliferation

To identify the key miRNA binding to hsa_circ_0038382, an online tool, CircInteractome, was used to predict miRNA binding to hsa_circ_0038382. Based on the CircInteractome prediction, 2 binding sites were found between hsa_circ_0038382 and miR-940 (Fig. 3A). After performing a luciferase assay to identify the binding sites, the miR-940 mimic induced a 50% decrease in luciferase activity in the hsa_circ_0038382-WT group, a 40% decrease in the hsa_circ_0038382-MUT1 group, and a 25% decrease in the hsa_circ_0038382-MUT2 group (Fig. 3B). However, the luciferase activity in the co-hsa_circ_0038382-MUT group was affected by the miR-940 mimic. Compared to normal skin tissues, the expression of miR-940 in keloid tissues showed a 5-fold elevation (Fig. 3C). The Pearson's correlation analysis showed that the expression of hsa_circ_0038382 was negatively correlated with miR-940 expression in keloid tissues ($R = -0.6620$, Fig. 3D). After the transfection of HKFs with the miR-940 mimic, the proliferation of HKFs was enhanced (Fig. 3E). These results prove that miR-940 could be targeted by hsa_circ_0038382 and contribute to the proliferation of HKFs.

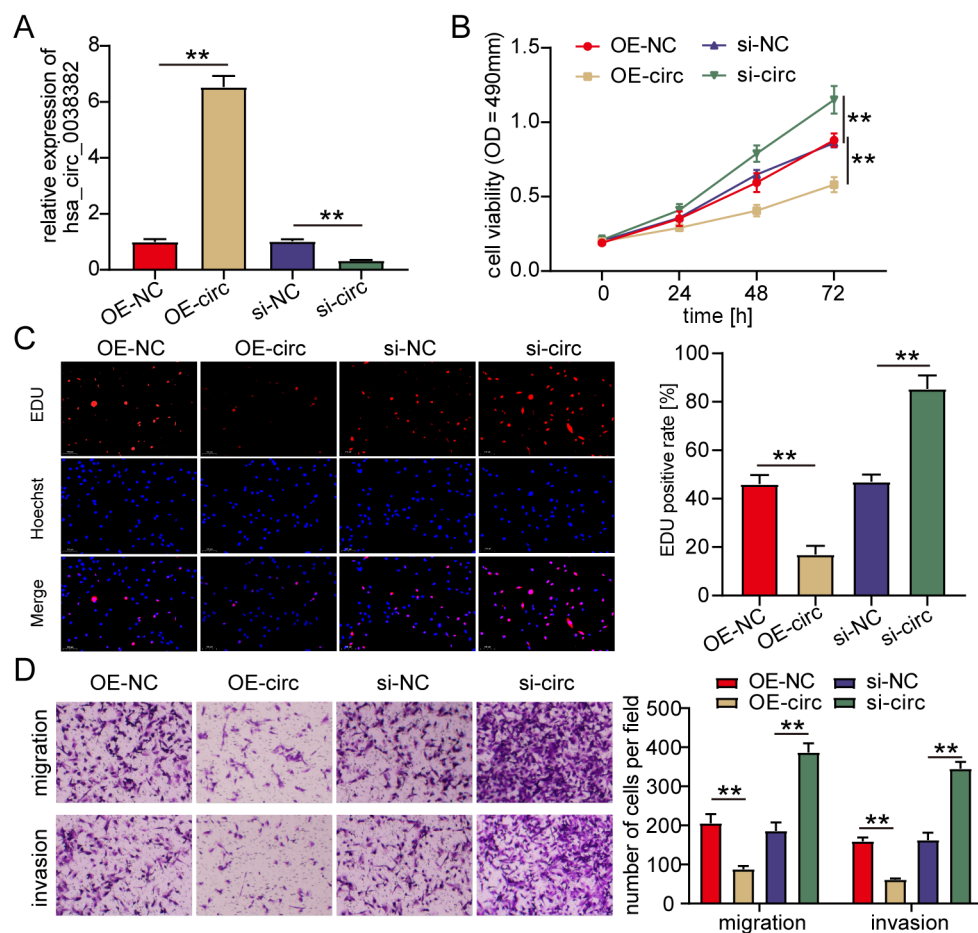


Fig. 2. The hsa_circ_0038382 attenuates keloid formation in vitro. A. Real-time quantitative reverse transcription polymerase chain reaction (qRT-PCR) identified the high transfection efficiency of hsa_circ_0038382 overexpression vectors and si-hsa_circ_0038382 vectors in human keloid fibroblasts (HKFs); B. Cell counting kit-8 (CCK-8) assays detected the effect of hsa_circ_0038382 on the proliferation of HKFs; C. The 5-ethynyl-2'-deoxyuridine (EdU) assays further detected the effect of hsa_circ_0038382 on the proliferation of HKFs; D. Transwell migration and invasion assays measured the effect of hsa_circ_0038382 on the migration and invasion of HKFs with the quantification of cell number at $\times 200$ magnification

OE-NC – negative control of hsa_circ_0038382 overexpression vector; OE-circ – hsa_circ_0038382 overexpression vector; si-NC – negative control of si-hsa_circ_0038382; si-circ – si-hsa_circ_0038382; OD – optical density; **p < 0.01.

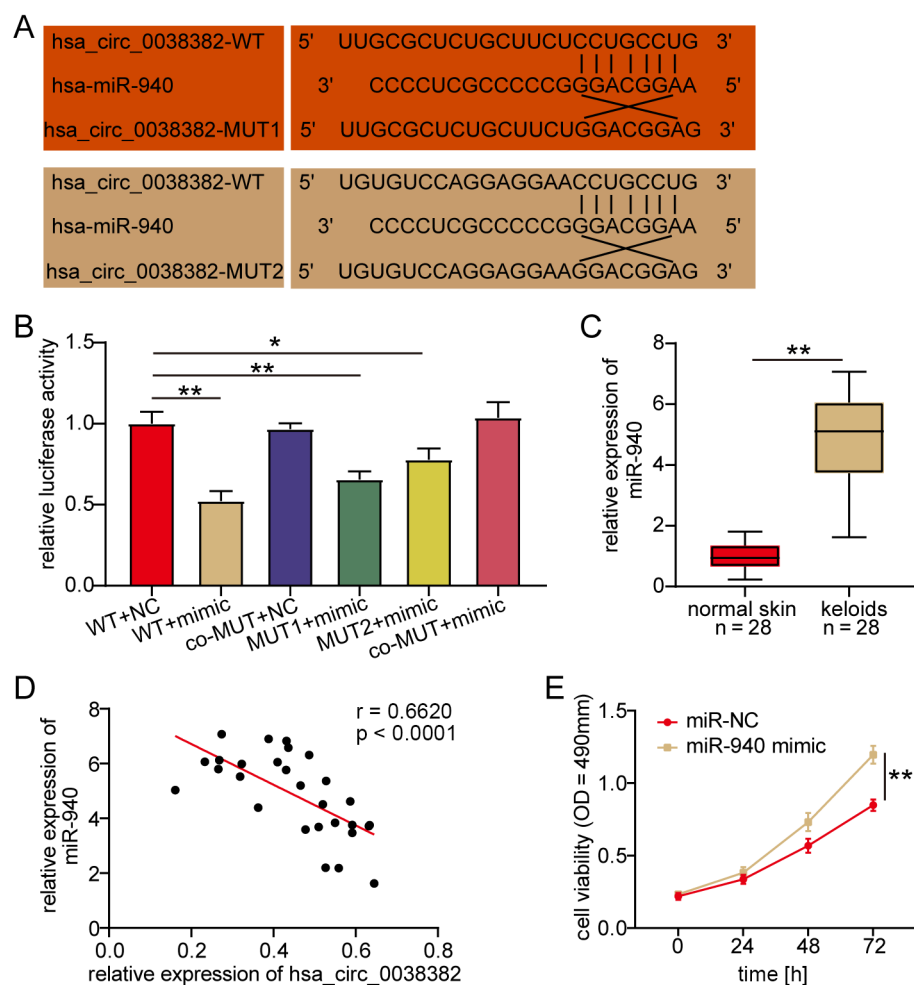


Fig. 3. The miR-940 targeted by hsa_circ_0038382 promotes human keloid fibroblast (HKF) proliferation.

A. CircInteractome predicted the binding sites between hsa_circ_0038382 and miR-940; B. Luciferase assay confirmed the binding sites between hsa_circ_0038382 and miR-940 in HKFs; C. Real-time quantitative reverse transcription polymerase chain reaction (qRT-PCR) confirmed the upregulation of miR-940 in keloid tissues, $n = 28$; D. Pearson's correlation analysis confirmed the negative correlation between hsa_circ_0038382 and miR-940 in keloid tissues; E. Cell counting kit-8 (CCK-8) assays revealed the positive effect of miR-940 on the proliferation of HKFs

WT – wild-type hsa_circ_0038382; MUT1 – mutant at site 1 of hsa_circ_0038382; MUT2 – mutant at site 2 of hsa_circ_0038382; co-MUT – mutant at site 1 and 2 of hsa_circ_0038382; NC – negative control of miR-940 mimic; + – co-transfection; miR-NC – negative control of miR-940 mimic; OD – optical density; * $p < 0.05$; ** $p < 0.01$.

TBX5, a target gene of miR-940, inhibits HKF proliferation

To explore the downstream regulators of miR-940, TargetScan, an online tool, was used to predict the target genes of miR-940. According to TargetScan predictions, there is a binding site between *TBX5* and miR-940 (Fig. 4A). The luciferase assay further confirmed the binding site between *TBX5* and miR-940, because the miR-940 mimic reduced the luciferase activity in the *TBX5*-WT group but did not affect the luciferase activity in the *TBX5*-MUT group (Fig. 4B). Compared with normal skin tissues, *TBX5* expression was significantly reduced in keloid tissues ($p < 0.01$, Fig. 4C). The Pearson's correlation analysis revealed a negative correlation between *TBX5* and miR-940 expression in keloid tissues ($R = -0.7279$, Fig. 4D), and a positive correlation between *TBX5* and hsa_circ_0038382 expression in keloid tissues ($R = 0.7335$, Fig. 4E). After the transfection of HKFs with *TBX5* overexpression vectors, the proliferation of HKFs declined (Fig. 4F). These data confirm that *TBX5* targeted by miR-940 promotes the proliferation of HKFs.

TBX5 overexpression reversed the effect of hsa_circ_0038382 knockdown on HKFs

Since *TBX5* acts downstream of the hsa_circ_0038382/miR-940 axis, we transfected HKFs with hsa_circ_0038382 knockdown with or without the *TBX5* overexpression vectors. Western blotting showed that the *TBX5* protein expression was inhibited by 50% in HKFs with hsa_circ_0038382 knockdown. However, *TBX5* overexpression vectors recovered the effects of hsa_circ_0038382 knockdown on *TBX5* protein expression (Fig. 5A). We performed cell functional experiments to explore whether *TBX5* could recover the effect of hsa_circ_0038382 on the proliferation, migration and invasion of HKFs. As shown in Fig. 5B, the increase in proliferation induced by si-hsa_circ_0038382 was reversed by the co-transfection with *TBX5* overexpression vectors in HKFs. The EdU assay further confirmed that the overexpression of *TBX5* recovered the increase in the EdU-positive rate caused by si-hsa_circ_0038382 (Fig. 5C). Similarly, the enhanced migration and invasion abilities of HKFs caused by hsa_circ_0038382 knockdown were impaired by the co-transfection with *TBX5* overexpression vectors (Fig. 5D). Cell function experiments identified that the positive effect of hsa_circ_0038382 downregulation on HKFs was reversed by the overexpression of *TBX5*.

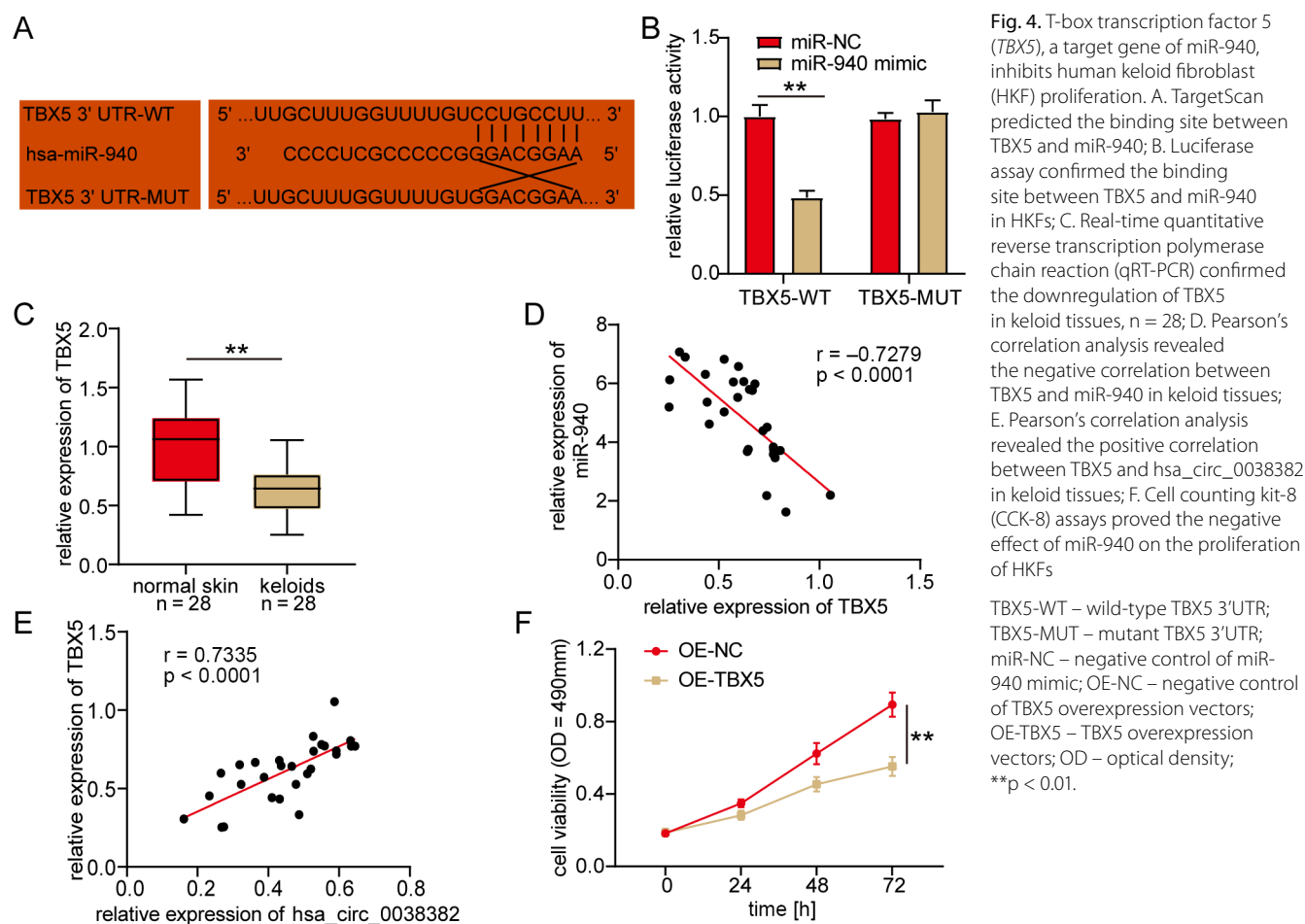


Fig. 4. T-box transcription factor 5 (TBX5), a target gene of miR-940, inhibits human keloid fibroblast (HKF) proliferation. **A.** TargetScan predicted the binding site between TBX5 and miR-940; **B.** Luciferase assay confirmed the binding site between TBX5 and miR-940 in HKFs; **C.** Real-time quantitative reverse transcription polymerase chain reaction (qRT-PCR) confirmed the downregulation of TBX5 in keloid tissues, $n = 28$; **D.** Pearson's correlation analysis revealed the negative correlation between TBX5 and miR-940 in keloid tissues; **E.** Pearson's correlation analysis revealed the positive correlation between TBX5 and hsa_circ_0038382 in keloid tissues; **F.** Cell counting kit-8 (CCK-8) assays proved the negative effect of miR-940 on the proliferation of HKFs

TBX5-WT – wild-type TBX5 3'UTR; TBX5-MUT – mutant TBX5 3'UTR; miR-NC – negative control of miR-940 mimic; OE-NC – negative control of TBX5 overexpression vectors; OE-TBX5 – TBX5 overexpression vectors; OD – optical density; ** $p < 0.01$.

Discussion

Recently, the circRNAs have been reported to participate in keloid formation.^{10,11,25} This study revealed that the novel circRNA, hsa_circ_0038382, was downregulated in keloid tissues and fibroblasts, and it enhanced the proliferation, migration and invasion abilities of keloid fibroblasts. Moreover, we showed that hsa_circ_0038382, miR-940 and TBX5 form a circRNA-miRNA-mRNA regulatory network to regulate keloid formation.

The circRNAs play key roles in multiple human diseases, although they do not code protein.^{26–28} Due to the rapid development of RNA sequencing technology, microarray analysis has been a good method for identifying key circRNAs in human diseases.²⁹ Zhang et al. applied high-throughput RNA sequencing technology and bioinformatic analysis and confirmed that the key circRNAs in keloids were hsa_circRNA_0008259, hsa_circRNA_0005480 and hsa_circRNA_0002198.³⁰ In this study, we achieved a circRNA microarray of keloids (GSE184097) from the GEO database and confirmed that hsa_circ_0038382 was downregulated in keloid samples. After transfecting hsa_circ_0038382 overexpression vectors or si-hsa_circ_0038382 into keloid fibroblasts, hsa_circ_0038382 was found to inhibit keloid formation, which uncovered the function of hsa_circ_0038382 in keloids for the first

time. Currently, the treatment of keloids includes surgical excision combined with radiotherapy, corticosteroids, pressure therapy, and other treatments.³¹ However, because of the high recurrence rate, no single treatment has been proven to be the most effective.⁶ We identified the abnormal expression of hsa_circ_0038382 in keloids. Its overexpression inhibited keloid formation. Our results suggested that hsa_circ_0038382 may be a biomarker for keloid prognosis, and emerging drugs targeting hsa_circ_0038382 may effectively inhibit keloid formation.

An increasing number of studies have reported that the regulatory network formed by circRNAs, miRNAs and mRNAs participates in biological processes such as cell proliferation,²⁷ cell apoptosis³² and cell differentiation.³³ Liu et al. confirmed the regulatory network formed by circPTPN12, miR-21-5p and SMAD7 in keloid fibroblasts, showing that circPTPN12 inhibits the growth of keloid fibroblasts by targeting miR-21-5p/AMAD7 axis.¹⁵ The circ_101238 targets the miR-138-5p/CDK6 axis, promoting the proliferation and inhibiting the apoptosis of keloid fibroblasts.⁹ In this study, we used keloid fibroblasts to confirm that hsa_circ_0038382 could bind miR-940 to upregulate the target gene (TBX5) of miR-940. In other words, hsa_circ_0038382, miR-940 and TBX5 formed the regulatory network to regulate keloid formation.

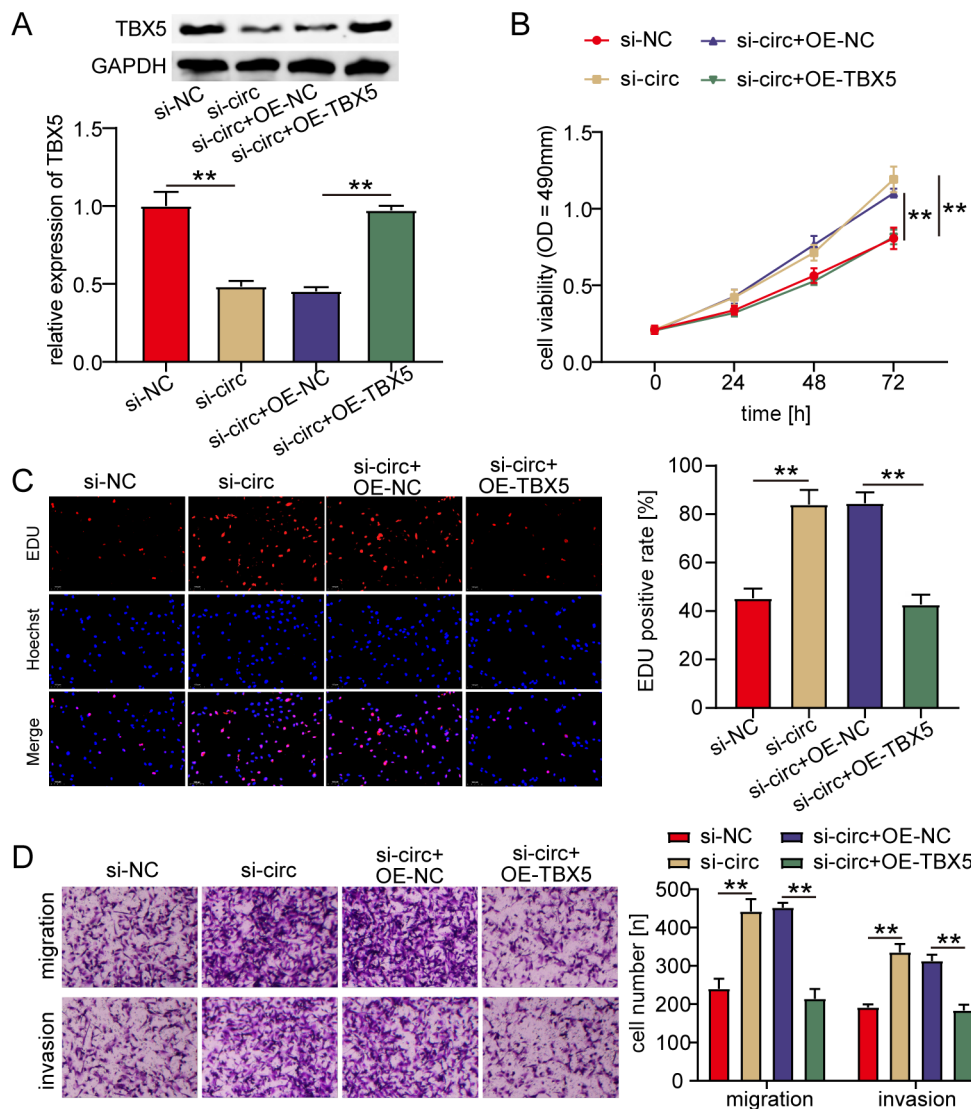


Fig. 5. Overexpression of T-box transcription factor 5 (TBX5) reversed the effect of hsa_circ_0038382 knockdown on human keloid fibroblasts (HKFs). A. Western blotting detected the expression of TBX5 protein in transfected HKFs; B,C. Cell counting kit-8 (CCK-8) assay (B) and 5-ethynyl-2'-deoxyuridine (EdU) assay (C) detected the proliferation of transfected HKFs; D. Transwell migration and invasion assays measured the abilities of migration and invasion of transfected HKFs with the quantification of cell number at x200 magnification

si-NC – negative control of si-hsa_circ_0038382; si-circ – si-hsa_circ_0038382; OE-NC – negative control of TBX5 overexpression vector; OE-TBX5 – TBX5 overexpression vector; GAPDH – glyceraldehyde 3-phosphate dehydrogenase; OD – optical density; **p < 0.01.

The role of miR-940 has been reported in multiple diseases, such as sepsis,³⁴ spinal cord injury³⁵ and cancer.³⁶ The overexpression of miR-940 has been shown to induce the progression of cervical cancer. However, its overexpression inhibits the malignancy of lung cancer.³⁷ These previous studies suggest different roles of miR-940 in various cancers. The effect of miR-940 on keloids as benign skin fibroproliferative tumors should be explored. Here, we confirmed that miR-940, downstream of hsa_circ_0038382, contributes to the proliferation of keloid fibroblasts. In addition, our study identified *TBX5* as the target gene of miR-940 in keloid fibroblasts.

The overexpression of TBX5 inhibits colony formation but induces cell apoptosis, thereby attenuating cell proliferation and invasion in tumor cells.^{20,21} In non-small cell lung carcinoma cells, low levels of TBX5 indicated poor tumor-node-metastasis (TNM) stages, histopathologic type and lymph node status. Additionally, the overexpression of TBX5 suppressed tumor growth in vivo.²² In cutaneous melanoma, TBX5 knockdown

promotes cutaneous melanoma cell proliferation, migration and invasion, suggesting an antitumor role of TBX5 in cutaneous melanoma. Similar to a previous study on TBX5 in other cancers, our study confirmed that the overexpression of *TBX5* inhibits the proliferation of keloid fibroblasts. In addition, in hsa_circ_0038382 knockdown experiments, the overexpression of *TBX5* restored the promotive effect of hsa_circ_0038382 in keloid fibroblasts.


Limitations


There are some limitations to our study. The study used the microarray analysis and cell function experiments to evaluate the effects of keloid formation, but the effect of the hsa_circ_0038382/miR-940/*TBX5* axis on keloid formation in vivo needs to be further investigated. Moreover, the clinical value of the hsa_circ_0038382/miR-940/*TBX5* axis needs to be explored by collecting more clinical samples.


Conclusions


This study, for the first time, demonstrated the inhibitory effect of hsa_circ_0038382 on keloids by suppressing the proliferation, migration and invasion of keloid fibroblasts. The miR-940/TBX5 was identified as the downstream regulator of hsa_circ_0038382 in keloid formation. Our results provide novel therapeutic targets in keloid prevention.

ORCID iDs

Meihong Cai  <https://orcid.org/0000-0002-4229-4399>

Zhen Hu  <https://orcid.org/0000-0002-0313-9513>

Lin Liu  <https://orcid.org/0000-0002-7945-9337>

Jiangwei Su  <https://orcid.org/0000-0001-9442-1399>

References

- Liu T, Ma X, Ouyang T, et al. Efficacy of 5-aminolevulinic acid–based photodynamic therapy against keloid compromised by downregulation of SIRT1–SIRT3–SOD2–mROS dependent autophagy pathway. *Redox Biol.* 2019;20:195–203. doi:10.1016/j.redox.2018.10.011
- Shi K, Qiu X, Zheng W, Yan D, Peng W. MiR-203 regulates keloid fibroblast proliferation, invasion, and extracellular matrix expression by targeting EGR1 and FGF2. *Biomed Pharmacother.* 2018;108:1282–1288. doi:10.1016/j.biopha.2018.09.152
- Jfri A, O'Brien E, Alavi A, Goldberg SR. Association of hidradenitis suppurativa and keloid formation: A therapeutic challenge. *JAAD Case Rep.* 2019;5(8):675–678. doi:10.1016/j.jidcr.2019.06.001
- Lee S, Kim SK, Park H, et al. Contribution of autophagy–Notch1-mediated NLRP3 inflammasome activation to chronic inflammation and fibrosis in keloid fibroblasts. *Int J Mol Sci.* 2020;21(21):8050. doi:10.3390/ijms21218050
- Lee H, Jang Y. Recent understandings of biology, prophylaxis and treatment strategies for hypertrophic scars and keloids. *Int J Mol Sci.* 2018;19(3):711. doi:10.3390/ijms19030711
- Bojanic C, To K, Hatoum A, et al. Mesenchymal stem cell therapy in hypertrophic and keloid scars. *Cell Tissue Res.* 2021;383(3):915–930. doi:10.1007/s00441-020-03361-z
- Shin JY, Yun SK, Roh SG, Lee NH, Yang KM. Efficacy of 2 representative topical agents to prevent keloid recurrence after surgical excision. *J Oral Maxillofac Surg.* 2017;75(2):401.e1–401.e6. doi:10.1016/j.joms.2016.10.009
- Kristensen LS, Andersen MS, Stagsted LVW, Ebbesen KK, Hansen TB, Kjems J. The biogenesis, biology and characterization of circular RNAs. *Nat Rev Genet.* 2019;20(11):675–691. doi:10.1038/s41576-019-0158-7
- Yang D, Li M, Du N. Effects of the circ_101238/miR-138-5p/CDK6 axis on proliferation and apoptosis keloid fibroblasts. *Exp Ther Med.* 2020;20(3):1995–2002. doi:10.3892/etm.2020.8917
- Wang B, Yin H, Zhang H, Wang T. CircNRP1 facilitates keloid progression via FXR1-mediated upregulation of miR-503-3p and miR-503-5p. *Int J Mol Med.* 2021;47(5):70. doi:10.3892/ijmm.2021.4903
- Shi J, Yao S, Chen P, et al. The integrative regulatory network of circRNA and microRNA in keloid scarring. *Mol Biol Rep.* 2020;47(1):201–209. doi:10.1007/s11033-019-05120-y
- Liu J, Xue N, Guo Y, et al. CircRNA_100367 regulated the radiation sensitivity of esophageal squamous cell carcinomas through miR-217/Wnt3 pathway. *Aging.* 2019;11(24):12412–12427. doi:10.18632/aging.102580
- Yu L, Liu Y. CircRNA_0016624 could sponge miR-98 to regulate BMP2 expression in postmenopausal osteoporosis. *Biochem Biophys Res Commun.* 2019;516(2):546–550. doi:10.1016/j.bbrc.2019.06.087
- Li H, Xu JD, Fang XH, et al. Circular RNA circRNA_000203 aggravates cardiac hypertrophy via suppressing miR-26b-5p and miR-140-3p binding to Gata4. *Cardiovasc Res.* 2020;116(7):1323–1334. doi:10.1093/cvr/cvz215
- Liu F, Li T, Zhan X. Silencing circular RNAPTNP12 promoted the growth of keloid fibroblasts by activating Wnt signaling pathway via targeting microRNA-21-5p. *Bioengineered.* 2022;13(2):3503–3515. doi:10.1080/21655979.2022.2029108
- Zhang H, Peng J, Lai J, et al. MiR-940 promotes malignant progression of breast cancer by regulating FOXO3. *Biosci Rep.* 2020;40(9):BSR20201337. doi:10.1042/BSR20201337
- Zhou Z, Xu YP, Wang LJ, Kong Y. MiR-940 potentially promotes proliferation and metastasis of endometrial carcinoma through regulation of MRV11. *Biosci Rep.* 2019;39(6):BSR20190077. doi:10.1042/BSR20190077
- Gu GM, Zhan YY, Abuduwaili K, et al. MiR-940 inhibits the progression of NSCLC by targeting FAM83F. *Eur Rev Med Pharmacol Sci.* 2018;22(18):5964–5971. doi:10.26355/eurrev_201809_15927
- Wang H, Song T, Qiao Y, Sun J. MiR-940 inhibits cell proliferation and promotes apoptosis in esophageal squamous cell carcinoma cells and is associated with post-operative prognosis. *Exp Ther Med.* 2019;19(2):833–840. doi:10.3892/etm.2019.8279
- He ML, Chen Y, Peng Y, et al. Induction of apoptosis and inhibition of cell growth by developmental regulator hTBX5. *Biochem Biophys Res Commun.* 2002;297(2):185–192. doi:10.1016/S0006-291X(02)02142-3
- Yu J, Ma X, Cheung KF, et al. Epigenetic inactivation of T-box transcription factor 5, a novel tumor suppressor gene, is associated with colon cancer. *Oncogene.* 2010;29(49):6464–6474. doi:10.1038/ncr.2010.370
- Ma R, Yang Y, Tu Q, Hu K. Overexpression of T-box transcription factor 5 (TBX5) inhibits proliferation and invasion in non-small cell lung carcinoma cells. *Oncol Res.* 2017;25(9):1495–1504. doi:10.3727/096504017X14883287513729
- Dong X, Wang Y, Qu Y, Liu J, Feng X, Xu X. MicroRNA-603 promotes progression of cutaneous melanoma by regulating TBX5. *Comput Math Methods Med.* 2021;2021:1888501. doi:10.1155/2021/1888501
- Livak KJ, Schmittgen TD. Analysis of relative gene expression data using real-time quantitative PCR and the 2^{−ΔΔCT} method. *Methods.* 2001;25(4):402–408. doi:10.1006/meth.2001.1262
- Wang J, Wu H, Xiao Z, Dong X. Expression profiles of lncRNAs and circRNAs in keloid. *Plast Reconstr Surg Glob Open.* 2019;7(6):e2265. doi:10.1097/GOX.0000000000002265
- Li X, Ding J, Wang X, Cheng Z, Zhu Q. NUDT21 regulates circRNA cyclization and ceRNA crosstalk in hepatocellular carcinoma. *Oncogene.* 2020;39(4):891–904. doi:10.1038/s41388-019-1030-0
- Huang Z, Ma W, Xiao J, Dai X, Ling W. CircRNA_0092516 regulates chondrocyte proliferation and apoptosis in osteoarthritis through the miR-337-3p/PTEN axis. *J Biochem.* 2021;169(4):467–475. doi:10.1093/jb/mvaa119
- Chang X, Zhu G, Cai Z, et al. MiRNA, lncRNA and circRNA: Targeted molecules full of therapeutic prospects in the development of diabetic retinopathy. *Front Endocrinol.* 2021;12:771552. doi:10.3389/fendo.2021.771552
- Li S, Teng S, Xu J, et al. Microarray is an efficient tool for circRNA profiling. *Brief Bioinform.* 2019;20(4):1420–1433. doi:10.1093/bib/bby006
- Zhang Z, Yu K, Liu O, et al. Expression profile and bioinformatics analyses of circular RNAs in keloid and normal dermal fibroblasts. *Exp Cell Res.* 2020;388(1):111799. doi:10.1016/j.yexcr.2019.111799
- Ojeh N, Bharatha A, Gaur U, Forde AL. Keloids: Current and emerging therapies. *Scars Burns Heal.* 2020;6:205951312094049. doi:10.1177/2059513120940499
- Ly YS, Wang C, Li LX, Han S, Li Y. Effects of circRNA_103993 on the proliferation and apoptosis of NSCLC cells through miR-1271/ERG signaling pathway. *Eur Rev Med Pharmacol Sci.* 2020;24(16):8384–8393. doi:10.26355/eurrev_202008_22635
- Chen X, Ouyang Z, Shen Y, et al. CircRNA_28313/miR-195a/CSF1 axis modulates osteoclast differentiation to affect OVX-induced bone absorption in mice. *RNA Biol.* 2019;16(9):1249–1262. doi:10.1080/15476286.2019.1624470
- Zhang S, Wei Y, Liu J, Zhuang Y. MiR-940 serves as a diagnostic biomarker in patients with sepsis and regulates sepsis-induced inflammation and myocardial dysfunction. *J Inflamm Res.* 2021;14:4567–4574. doi:10.2147/JIR.S316169
- Wang B, Shen PF, Qu YX, et al. MiR-940 promotes spinal cord injury recovery by inhibiting TLR4/NF-κB pathway-mediated inflammation. *Eur Rev Med Pharmacol Sci.* 2019;23(8):3190–3197. doi:10.26355/eurrev_201904_17677
- Hou L, Chen M, Yang H, et al. MiR-940 inhibited cell growth and migration in triple-negative breast cancer. *Med Sci Monit.* 2016;22:3666–3672. doi:10.12659/MSM.897731
- Jiang K, Zhao T, Shen M, et al. MiR-940 inhibits TGF-β-induced epithelial-mesenchymal transition and cell invasion by targeting Snail in non-small cell lung cancer. *J Cancer.* 2019;10(12):2735–2744. doi:10.7150/jca.31800